Sensitivity analysis of the Propagation of the Low Sonic Boom to the aerology

Patrice Malbéqui, Pierre-Elie Normand, Louis Budin, Gérald Carrier

SENSITIVITY ANALYSIS OF THE PROPAGATION OF LOW SONIC BOOM TO THE AEROLOGY

P. Malbéqui[1] P.-E. Normand[2] L. Budin[3] G. Carrier[1]
[1]ONERA, Châtillon, France
[2]Dassault Aviation, Saint-Cloud, France
[3]Master degree, Sciences Sorbonne Université, France
patrice.malbequi@onera.fr

ABSTRACT

Several concepts of supersonic commercial aircraft are emerging and most of them aim at flying over land. The main obstacle for the development of a supersonic aircraft remains the loud and sudden sonic boom felt by the population overflown during the cruise. As low boom designs gain in maturity an acceptable sound level for the sonic booms could be reached. However the acceptability level has still be defined by the regulation authorities as well as the means to evaluate it. The sonic boom sound level on the ground depends on the nearfield signature of the aircraft together with the state of the atmosphere it goes through. This paper examines the influence of the aerology on a low boom signature. The propagation is predicted using the eikonal equation. The aerology is provided by the Integrated Global Radiosonde Archive database, from which one thousand atmospheric profiles altogether have been extracted at 24 locations all over the world. This database contains a representative set of atmospheres, allowing a code-to-code benchmarking. The comparisons done in a collaborative effort with Dassault Aviation and ONERA are in a quite good agreement. Disparities can be explained through the analysis of numerical method implemented in the codes. The sensitivity analysis of the propagation of the sonic boom shows that, despite dispersions on the aerology, the maximum overpressure and the rise time of the pressure signal are close together. In contrast, the extent of the carpet, derived from the cut-off rays on the ground, exhibits a larger deviation.

1. INTRODUCTION

Unlike procedures used for subsonic aircraft, where ground noise measurements could be backward-propagated to the aircraft source and then forward-propagated for prediction in prescribed reference conditions, the sonic boom generated by a supersonic aircraft does not enable us such an approach due to nonlinearities and strong atmosphere effects during long range sound propagation.

As specified in the European RUMBLE project [1], future sonic boom regulation and certification scheme will rely heavily on simulation. As a result, in addition to measurements, the sonic boom prediction will have to play a key role in the future supersonic certification process. Henceforth, prediction capabilities with high level of accuracy is requested regarding both near-field air flow field and ground far-field pressure signature. The RUMBLE activities on the sonic boom prediction capabilities include several items:

- to validate the numerical methods for sonic boom prediction, to accurately characterize the near-field signature and predict the sonic boom effects on ground using experimental data from wind tunnel near-field measurements, flight tests data, and code-to-code verification,
- to validate wind tunnel techniques for high accuracy near-field signature measurement in cruise conditions,
- to develop and validate models for indoor sonic boom prediction accounting for building response,
- to design the aerodynamic shape of a low boom demonstrator for the preliminary design of a low boom demonstrator,
- to provide recommendations on sonic boom prediction process complying with certification procedures.

This paper deals with the prediction of the propagation in the atmosphere from the aircraft to the ground, generated by a low boom concept. The main physical phenomena are addressed using the ray method. The influence of the turbulence in the Planetary Boundary Layer is neglected.

Section 2 summarizes the theoretical background of the ray method, focusing on the techniques and taking into account the specificities of the sonic boom. Comparisons between the codes BANGV and DABANG used by ONERA and Dassault Aviation, respectively, are presented in Section 3, including the configurations of the ISO-Standard atmosphere and the IGRA database. Section 4 describes the sensitivity analysis of the propagation of the sonic boom on the ground, performed through the various conditions available in the IGRA database.

2. THEORETICAL BACKGROUND ON PROPAGATION OF THE SONIC BOOM

The main specificities of the two codes DABANG and BANGV for predicting the signature are listed below, more details can be found in [2] to [4]. The codes allow for sonic boom propagation under the following configurations:

- Any shape of the aircraft is possible; the near-field signature can be modeled by the so-called Whitham *F* function or with a cylindrical pressure distribution

at a given distance of the aircraft, derived from the CFD or the wind tunnel measurements.

- Various aircraft trajectories can be handled, such as cruise, maneuver and acceleration.
- A stratified meteorology without turbulence (no temporal fluctuations in the media during the propagation) is assumed, with profiles of temperature, wind, relative humidity and density. The interpolation is done using cubic splines.
- A flat and absorbing ground is considered, using the 4 parameters model proposed by Attenborough [6].

The two codes are based on the same ray theory, stating that the sound propagating along rays can be determined according to the Fermat principle. This theory is the well-known high frequency approximation, assuming locally plane wave propagation. The amplitude of the wave form is predicted along rays, through the cross-section of the ray-tube, using the Blokhintzev principle. The numerical implementation follows the formulation derived by Candel [5]. It is based on the integration of a system of 13 Partial Differential Equations: 4 PDEs to determine the rays, 8 PDEs to estimate the ray-tube cross-section, and 1 PDE for the nonlinear age variable.

To account for the non-linearity of the propagation in the atmosphere, due to the significant magnitude of the peak overpressure in the sonic boom, the codes solve the non-linear Burgers's equation, governing the distortion of the signal, associated with an appropriate technique to automatically handle the shock position. The acoustical absorption due to the thermo-viscous effects and the molecular relaxation of nitrogen and oxygen molecules is performed using a split-step algorithm.

3. CODE-TO-CODE COMPARISON

Dassault Aviation and ONERA use the codes presented in the previous Section, to validate the capability of the ray method to account for the main physical phenomena affecting the atmospheric propagation of a sonic boom signal, representative of a low-boom aircraft signature. The signal used as the common input is the near-field pressure signal from the NASA C25D low boom concept (see Figure 1). This concept corresponds to the NASA low boom flight demonstrator defined in the 2nd AIAA Sonic Boom Prediction Workshop. It is the result of the prediction using a Reynolds-averaged Navier-Stokes (RANS) computation at flight unit Reynolds number of 5.7 million per meter. Details of the comparison exercise done at Computational Aero-sciences Branch, NASA Langley and Ames Research Centers can be found in [8].

The aircraft trajectory is defined as follows: the cruise Mach number is assumed to be constant (no acceleration) and equals 1.6; 0° and 180° heading angles are considered, and the altitude of the aircraft is 15760 meter.

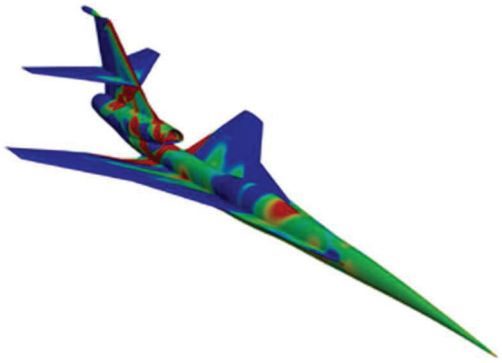

Figure 1. Nearfield signature on the aircraft, NASA C25 low boom Concept [8].

The nearfield signature used to initialize the ray codes under track (azimuthal angle of zero degree), is plotted in Figure 2 . The propagation starts at the reduced range R/L = 3, where R is the 330 feet and L is the 110 feet body length.

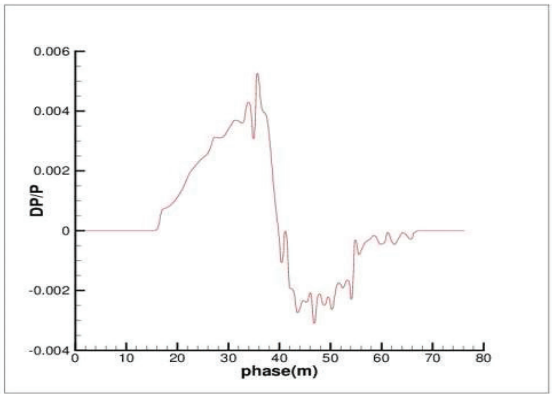

Figure 2. Near field signature under track, R/L = 3, NASA C25 low boom Concept.

The capability to predict the sonic boom primary carpet, as well as the sonic boom signatures over this carpet, is presented for various atmospheric conditions and a given aircraft trajectory, according to the test cases defined in RUMBLE [7].

The ISO-Standard atmosphere (ICAO 7488/3, 1993) with a constant 70 % relative humidity is first considered. Figure 3 illustrates the temperature and the density profiles.

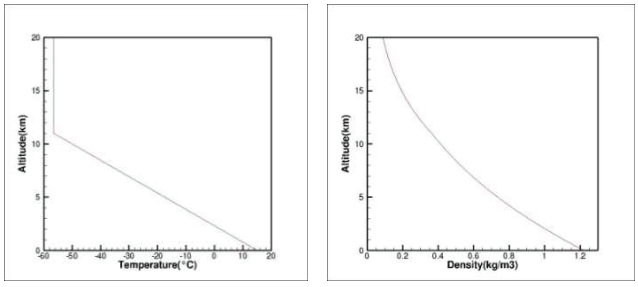

Figure 3. ISO-Standard atmosphere: temperature and density profiles.

Figure 4 shows a quite good agreement between the two codes of the signature predicted undertrack, both in terms of magnitudes of the positive and negative overpressure of the shocks as well as the rise time.

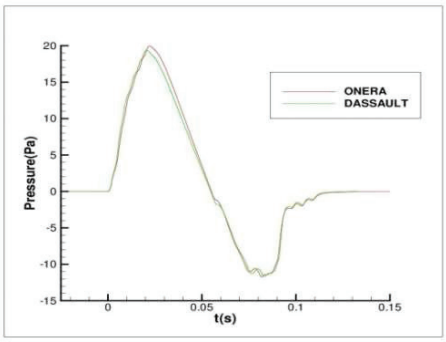

Figure 4. Signature on the ground undertrack for ISO-standard atmosphere. Dassault Aviation and ONERA predictions.

The atmospheric condition from the Integrated Global Radiosonde Archive available on line is now considered [9]. Data for the whole month of August 2012 from a subset of 24 locations in the world have been assembled by NASA and transformed into a HDF5 Format, to be used by RUMBLE partners. Figure 5 indicates the 24 locations from which data was extracted from IGRA.

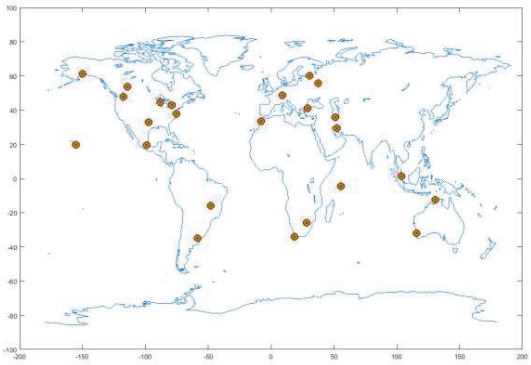

Figure 5: 24 Locations all over the word from the IGRA data base.

The objective is to compare: the cut-off angles, the positive and negative overpressures on the ground, and the metrics: ASEL, BSEL, CSEL, and PL values. The comparison is done by looking at histograms of the absolute difference between the values produced by the two propagation codes. The histogram's number of equally distributed bins is set with the hypothesis that the probability distribution function associated with code-to-code comparison should be Gaussian-like; therefore, the Scott's normal reference [13] rule can be used. For pressure and sound metrics we set the standard deviation to be a third of the expected precision, for cut-off angle comparison this criterion is relaxed because of the scarcity of the results.

Values of the bin-width and expected precision are presented in Table 1.

	Cut-off angle	Pressure	Sound metrics
Bin-width	0.2°	0.02 Pa	0.04 (dB)
Expected precision	±0.2°	±0.25 Pa	±0.3 (dB)

Table 1. Bin-width and expected precision on the predictions by the ray method.

Figure 6 and Figure 7 show the statistical comparisons between DABANG and BANGV for 794 atmospheres, on the cut-off angles, the overpressures, and the metrics, for an aircraft heading east. The expected precisions from Table 1 are represented with vertical red lines. By convention, positive values imply that the BANGV result is greater than the DABANG result, and for negative overpressure and minimum cut-off angle the opposite is implied.

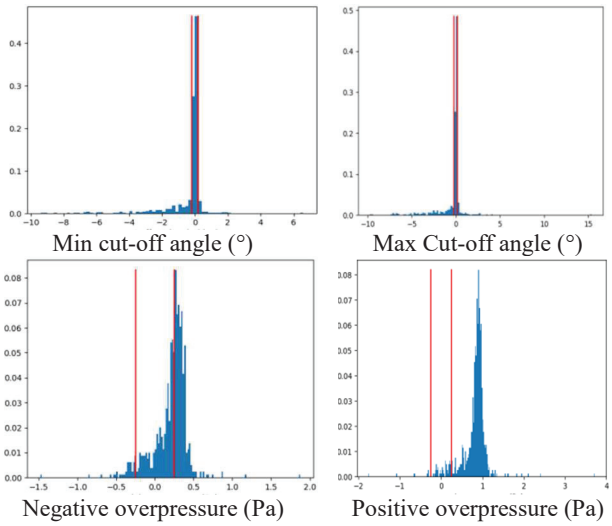

Figure 6. Histograms of the difference between BANGV and DABANG, aircraft heading east. Cut-off angles and overpressures.

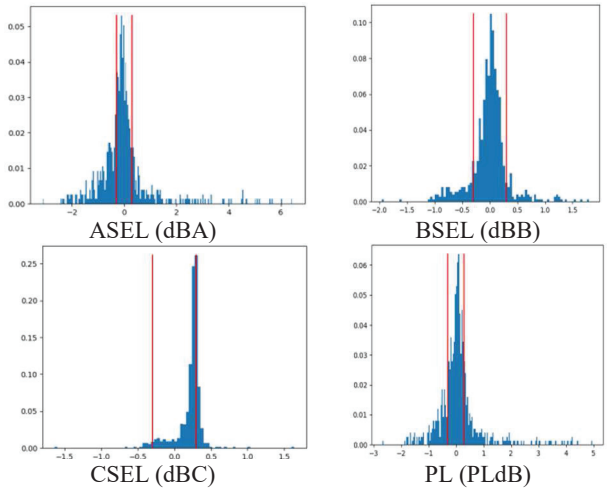

Figure 7. Histograms of the difference between BANGV and DABANG, aircraft heading east. Metrics: ASEL, BSEL, CSEL and PL.

Similarly, Figure 8 and Figure 9 show the statistical comparisons between DABANG and BANGV for 808 atmospheres, for an aircraft flying west.

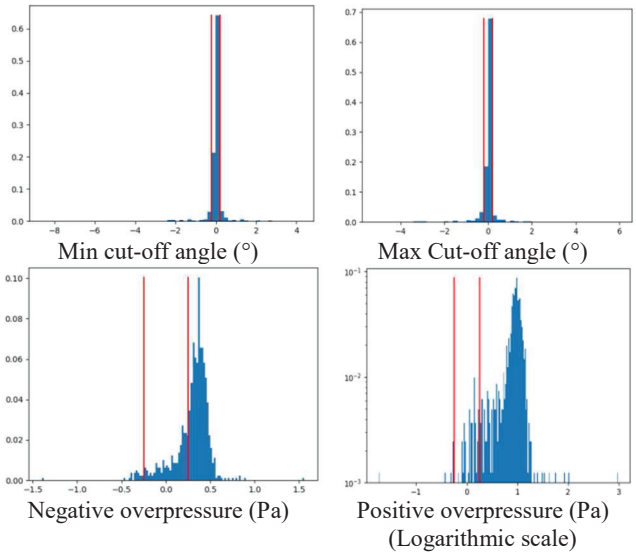

Figure 8. Histograms of the difference between BANGV and DABANG, aircraft heading west. Cut-off angles and overpressures.

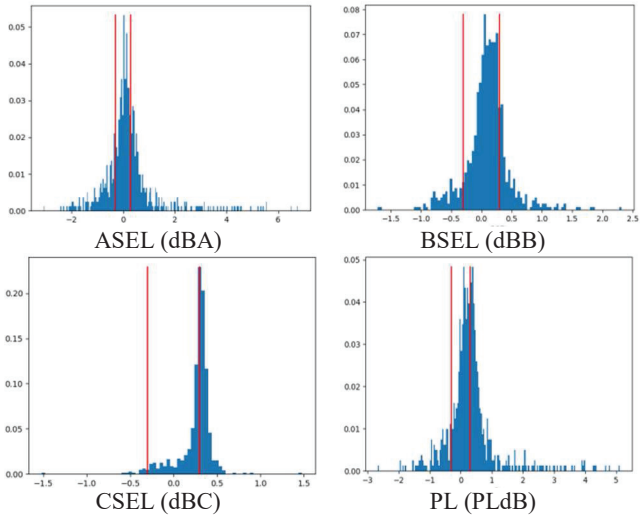

Figure 9. Histograms of the difference between BANGV and DABANG, aircraft heading west: ASEL, BSEL, CSEL and PL.

Concerning differences in cut-off angle, as much for west heading than east, more than 60% of the time the comparison is within the expected precision. However a non-negligible number of comparison points are largely off precision. Moreover BANGV statistically predicts a narrower carpet. The source of this discrepancy has been identified and comes from the difference in methodology used to determine cut-off angles in the two codes. In DABANG a ray is considered out of the cut-off zone as soon as the ray is refracted upwards ($z(t+dt) > z(t)$, with $z(t)$ the altitude of the ray at time t) and a bisection method is used to determine the maximum and minimum angle for which the ray is not refracted upwards. In BANGV an analytical solution of the cut-off angle is implemented for which in some cases the solution differs largely from the geometrical definition of the cut-off angle. BANGV now implements the two methodologies.

In terms of pressure differences most of the points are outside the expected precision, this is particularly noticeable in the histogram in logarithmic scale shown in figure 8. BANGV predicts most of the time higher positive overpressure and lower negative overpressure. It is interesting to see that this statistical bias is reflected differently amongst metrics.

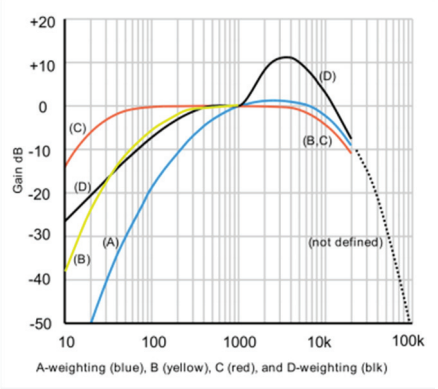

Figure 10. Weighting for metric ASEL, BSEL and CSEL (credit Peter J Skirrow).

Because of the weighting of the low frequency content from ASEL, BSEL and PL the bias is lowered and the difference distribution tends to be more centered unlike CSEL which maintains the bias towards higher values for the BANGV code.

The difference observed is suspected to come from different implementation of the acoustical absorption model. Further investigations are ongoing to determine the difference of absorption and dispersion values given by the model during the ray propagation between the two codes.

We now focus on the cut-off angles for the two locations ANCHORAGE and PRETORIA, where the largest differences between the two codes were observed. While the overpressure differences between DABANG and BANGV do not exceed one Pa, as shown on Table 3 and Table 3, the deviation in the cut-off angles can reach up to 5 degrees. It is here assumed that for these locations, where the impact of the lateral ray on the ground is sensitive to the conditions of the atmosphere, the two different techniques implemented in the codes may explain the differences. In DABANG the impact point is processed using a bisection algorithm, while in BANGV, under downward refracting atmosphere, the emission angle of an horizontal ray can be determined numerically by relating the emission angle, here straightforwardly computed, to the altitude at which the ray remains horizontal [4].

	min cut-off (°)	Max cut-off angle (°)
BANGV	-48.53	50.35
DABANG	-52.43	54.92

Table 2. ANCHORAGE: 50 meter altitude, run 1346328000, August the 30th 2002, at 12:00.

	Min cut-off angle(°)	Max cut-off angle (°)
BANGV	-48.53	50.35
DABANG	-52.43	54.92

Table 3. PRETORIA: 1523 meter altitude, run 1343815200, August the 1st 2002, at 10:00 AM.

4. INFLUENCE OF THE METEOROLGY ON THE LOW BOOM SIGNATURE

Previous studies have already analyzed in details the influence of the meteorology on sonic boom propagation. Along the ground track of a Paris to New York trip, close to those used for Concorde, including an aircraft acceleration [10]. Using the Whitham's F-functions, where the source term is adapted from an Airbus mock-up of a planned European Supersonic Commercial Transport designed for carrying 250 passengers at Mach 2 in cruise [11]; for a hypersonic Mach 6 cruise aircraft [12]. In this paper, the sensitivity of the aerology is dedicated to the low boom concept. It is first detailed for the influence of the aerology at Stuttgart in Germany, where an amount of 56 atmospheres are available, allowing a relevant statistical study. Figure 11 plots the profiles of the magnitude of the wind speed, the temperature, the relative humidity and the density.

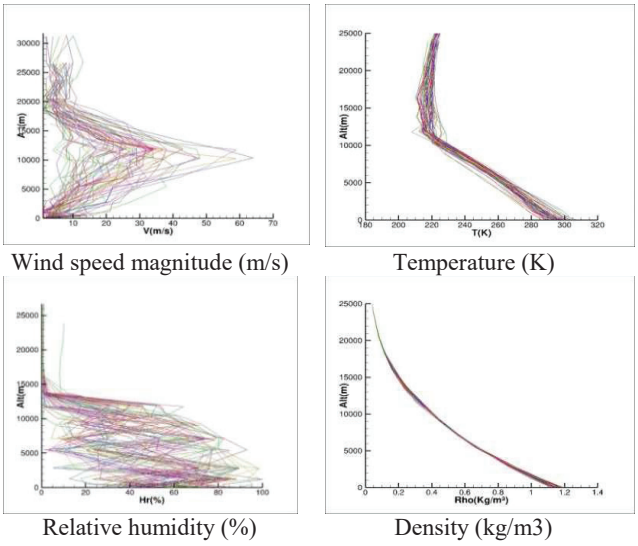

Wind speed magnitude (m/s) | Temperature (K)

Relative humidity (%) | Density (kg/m3)

Figure 11. Set of 56 aerology profiles at Stuttgart, Germany.

The relative humidity points out a great day to day variability on the whole runs. The wind speed profiles also show strong variability, with an increase close to 10000 meters, coherent with prevailing westerlies occurring at latitudes between 30 and 60 degrees. In contrast, as expected, the density and the temperature profiles decrease with the altitude with only weak differences between the runs. The temperature decreases typically by 5 degrees °K per km up 12 000 meter, then temperature when reaching the tropopause is roughly constant, and equals 220 °K, due to the disappearance of the atmosphere and the ozone layer. Figure 12 shows the ground carpet pattern (blue curve) and the width of the carpet (red line) of the sonic boom, determined by the two cut-off angles. Under ISO-Standard atmosphere, without speed, the carpet is symmetrical to the trajectory axis of the aircraft, while in the real atmosphere, in presence of a transverse wind, an asymmetry may occur. Then, differences may also appear depending on heading of the aircraft.

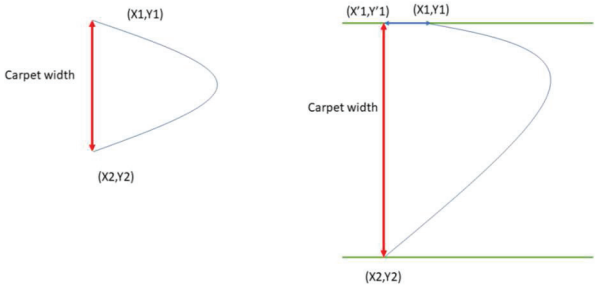

Figure 12. Definition of the width carpet. Left: ISO-Atmosphere; right: real atmosphere.

Table 4 summarizes the prediction of the mean value, $\hat{m} = \sum_{k=1}^{N} x_k$, and the standard deviation, $\hat{\sigma} = \sqrt{\sum_{k=1}^{N} |x_k - m_x|^2}$, where x_k represents a sample of the positive overpressure, the Rise Time and the carpet width over the N samples at Stuttgart, and for the 0° heading angle of the aircraft trajectory. It is observed that the standard deviation of overpressure and rise time remains weak, typically a few percent of the mean value, while for the width of the carpet it can reach 10 %.

over pressure (Pa)		Rise Time (s)		Carpet width (km)	
$\hat{m}$	$\hat{\sigma}$	$\hat{m}$	$\hat{\sigma}$	$\hat{m}$	$\hat{\sigma}$
19.5	0.5	$1.4\ 10^{-2}$	10^{-3}	55	8

Table 4. Mean and standard deviation of the overpressure, rise time and carpet width at Stuttgart.

Figure 13 finally summarizes the mean values and the standard deviation of the overpressure and the rise time propagated under track, and the width carpet, for the whole locations. In practice the number of samples for a given location typically varies from 10 to 60, so that the total number of samples is about one thousand. For Shiraz, only one sample is available so that no standard deviation is computed. On the right hand side of the graphic, STD and 0-STD bars correspond to ISO-Standard atmosphere results with and without atmospheric absorption, respectively.

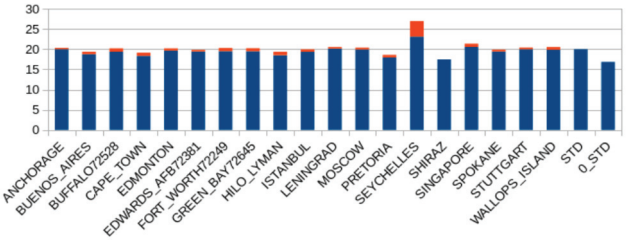

a) Overpressure (Pa)

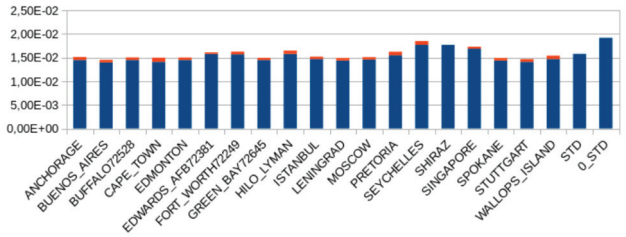

b) Rise time (s)

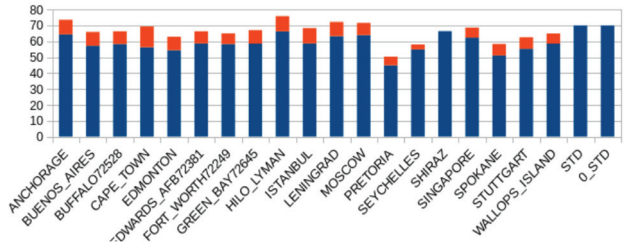

c) Carpet width (km)

Figure 13. : mean value, : standard deviation, whole locations extract from the IGRA data base.

In general, for each location, the same tendencies as in Stuttgart can be observed: the standard deviation of overpressure and rise time remains small. Moreover comparing the whole locations, except at Seychelles, weak variations of the mean value arise: the overpressure varies from 17 to 20 Pa and the rise time varies in the range 1.4 to 1.6 10^{-2} s. In contrast, the variability of the width carpet, which strongly depends on the wind speed, is more significant. While this study is restricted to the aerology encountered during August, its general tendency is in agreement with the one observed in [11], where it was observed that the variability is low undertrack, and is higher for lateral angles in terms of carpet width and boom amplitude.

5. CONCLUSION

A satisfactory agreement on the shape of the signature under track is found, especially the positive and negative overpressure and the rise time, between the two codes DABANG at BANGV, both based on the ray method. Differences in the width of the carpet can be observed for a few locations. This can be explained by the presence of nearly horizontal rays along the ground, where the prediction of the impact is sensitive to the algorithm implemented in each code to find the cut-off rays. This aspect, encountered for a set of singular configurations is investigated by comparing the ray trajectories and the age function. It is assumed that, when solving the same equations, the same results are expected. However for this kind of situations, the assumption of the ray method itself is no more valid. CAA methods based on the Euler's equations taking into account the scattering effect and turbulence of the Planetary Boundary Layer should provide more realistic results, with in contrast, a significant larger CPU time required.

The prediction on the propagation of the sonic boom shows that, despite disparities on the aerology and the climate related to the location, the over pressure and the rise time of the sonic bang on the ground remains close together, with typical standard deviations of a few Pa and 10^{-3} s, respectively.

Further analysis using various trajectories including manoeuvers and acceleration should be examined to extend the validity domain of the ray results.

6. ACKOWLEDGMENTS

This project has received funding from the European Union's Horizon 2020 research and innovation programme, under grant agreement No 769896.

7. REFERENCES

[1] https://rumble-project.eu/i/sites/default/files/Downloads/RUMBLE_brochure.pdf

[2] F. Dagrau: "Simulation de la propagation du bang sonique: de la CFD à l'acoustique non linéaire," Ph. D. Thesis, Sorbonne Université Paris 6 (Université Pierre et Marie Curie), 2009.

[3] R. Marchiano, F. Coulouvrat, and R. Grenon: "Numerical simulation of shock waves focusing at fold caustics, with application to sonic boom," *J. Acoust. Soc. Am.,* Vol. 114, pp.1758–1771, 2003.

[4] BANGV: *the Sonic Boom Software, User's Guide*, Version 4.0, December 2008.

[5] S. Candel: "Numerical solution of conservation equations arising in linear wave theory: application to aeroacoustics," *J. Fluid Mech.*, Vol. 83, pp. 465–493, 1977.

[6] K. Attenborough: "Acoustical impedance models for outdoor ground surfaces", *J. Sound Vib.*, Vol. 99, pp. 521-544, 1985.

[7] P. E. Normand and F. Dagrau: "Far field modeling validation – test cases specifications," RUMBLE Delivrable 2.3.1, September 2018.

[8] M. Park, M. Nemec: "Nearfield Summary and Statistical analysis of the second AIAA Sonic Boom prediction Workshop," 2nd AIAA Sonic Boom Prediction Worshop, Grapevine, Texas, USA, 7-8 January 2017.

[9] https://www.ncdc.noaa.gov/data-access/weather-balloon/integrated-global-radiosonde-archive

[10] R. Blumrich, F. Coulouvrat, D. Heimann: "Variability of focused sonic booms from accelerating supersonic aircraft in consideration of meteoroligcal effects", *J. Acoust. Soc. Am.* Vol. 118, No. 2, pp.696–706, 2005.

[11] R. Blumrich, F. Coulouvrat, D. Heimann: "Meteorologically induced variability of sonic boom characteristics of supersonic aircraft in cruising flight," *J. Acoust. Soc. Am.* Vol. 118, No. 2, pp.707–722, 2005.

[12] A. Loubeau, F. Coulouvrat: " Effects of meteorological variability on sonic boom propagation from hypersonic Aircraft", *AIAA Journal*, Vol. 47, No. 11, pp. 2632–2641, 2009.

[13] W. Scott: "On optimal and data-based histograms", Biometrika Vol 66, pp. 605-610, 1979.